Plasma Chemistry and Plasma Processing (2023) 43:1709–1729
https://doi.org/10.1007/s11090-023-10399-8

ORIGINAL PAPER

Plasma Treatment and Ozonation of Binary Mixtures: The Case of Maleic and Fumaric Acids

Volodymyr Shapoval[1] · Elisa Ceriani[1] · Diego Frezzato[1] · Cristina Paradisi[1] · Ester Marotta[1]

This paper is dedicated to the memory of Dr. Ulrich Kogelschatz, who honored us with his respect and friendship. Dr. Kogelschatz had extraordinary talents and a broad and deep scientific culture, which he generously shared with all who approached him. He is deeply missed.

Received: 15 July 2023 / Accepted: 18 September 2023 / Published online: 5 October 2023

Abstract
With respect to ozonation, plasma treatment involves direct contact between the discharge and the contaminated water therefore benefiting, in addition to ozone, also of short-lived reactive species. This paper focuses on mechanistic aspects of water treatment based on plasma activation (in-situ discharge) and ozonation (ex-situ discharge), using maleic acid and fumaric acid as model substrates and dielectric barrier discharges (DBDs) for producing plasma and ozone. Both types of experiments were carried out at different pH values and degradation profiles of residual concentration *vs* treatment time were compared in experiments in which each acid was treated individually and in mixture with the other. It was found that, under all conditions examined, plasma treatment was more efficient than ozonation for both acids, and that fumaric acid was always more reactive than maleic acid. Peculiar S-shaped degradation curves were obtained for the decay of maleic acid when treated in mixture with fumaric acid under acidic and neutral pH conditions in ozonation and in plasma experiments. This effect was not observed when maleic acid was treated in mixture with phenol instead of fumaric acid. The experimental data are nicely fitted with a simple kinetic model which assumes that a single reactive species, in steady state concentration, is responsible for the attack initiating the pollutants degradation. Based on the complete set of results obtained the conclusion is reached that, in the DBD reactor used, under acidic and neutral pH conditions ozone plays a major role in the degradation of maleic and fumaric acids also in direct plasma treatment.

Keywords Dielectric barrier discharge · Water treatment · Ozone · OH radical

Retired: Cristina Paradisi.

✉ Ester Marotta
ester.marotta@unipd.it

[1] Department of Chemical Sciences, University of Padova, Via Marzolo 1, 35131 Padua, Italy

Introduction

In 2003 Dr. Ulrich Kogelschatz, to whom this paper is dedicated, published the outstanding review article "Dielectric-Barrier Discharges: Their History, Discharge Physics, and Industrial Applications" which has since been cited over 2750 times. Among the various applications of dielectric-barrier discharges (DBD) described in the review, ozone production certainly stands out for diffusion and importance still nowadays for water decontamination, the topic of the present paper [1].

Water ozonation is carried out in two steps, ozone production in the actual ozonizer by DBD discharge followed by ozone mixing with the contaminated water to be treated [2]. As opposed to ozonation, which can be viewed as an "*ex-situ*" discharge-based process, direct plasma treatment involves production of the discharge in contact with the contaminated water ("in situ" discharge-based process) and offers the obvious advantage of possibly exploiting not only ozone but also more reactive short-lived species including notably OH radicals [3]. A variety of approaches has been proposed to implement *in-situ* discharge-based water treatment in many lab-scale prototypes and demonstration units, differing for the electrodes configuration and relative arrangement, the power supply, the reactor design just to cite the most important variables [3–7]. In our research we apply DBD discharges in air at atmospheric pressure and room temperature in contact with water and study the degradation of dissolved organic compounds. Notably, with the electrode configuration employed in our system, the discharge characteristics are not influenced by the solution conductivity and pH [8, 9]. Characterization of the pollutants degradation process is carried out by determining products, kinetics and the plasma generated reactive species involved [8–10]. Such mechanistic studies are propaedeutic to the development of technologies and applications.

Most useful insight into the processes activated by air plasma can be acquired from the comparison with results obtained in ozonation carried out under the same experimental conditions [11]. Ozone is one of the main reactive species produced in air plasma, by the well known reaction of atomic oxygen, originating from O_2 dissociation, with molecular oxygen (reactions 1–2) and, depending on the solution pH, decomposes more or less rapidly to form OH radicals [12–16], as detailed below.

$$O_2 + e^- \rightarrow O\left(^3P\right) + O\left(^1D\right) \tag{1}$$

$$O\left(^3P\right) + O_2 \rightarrow O_3 \tag{2}$$

Experiments performed recently in the DBD reactor used in the present work have demonstrated that if t-BuOH, a known quencher of $^{\bullet}OH$ which does not react with ozone [17], is added in large excess (5.0×10^{-2} M) to a phenol solution (5.0×10^{-4} M) and this mixture is subjected to plasma treatment, the decomposition of phenol is significantly slowed down by the competition for OH radicals by t-BuOH. Moreover, if t-BuOH is treated alone (5.0×10^{-4} M) with air plasma at pH 7.0, it is decomposed; on the contrary, if it is subjected to ozonation under the same conditions it does not react. One important fact which must be taken into account and that the above described experiments helped us clarify is that in air plasma experiments there

are two sources of OH radicals: one is plasma itself, in which •OH can be formed by dissociation of water (reaction 3) or by reaction of atomic oxygen with water (reaction 4) [1, 3], the other is the decomposition of ozone in water (reactions 5–10). As known from the literature, [12–16] this second process is favored at basic pH values.

$$H_2O + e^- \rightarrow {}^{\bullet}OH + {}^{\bullet}H \tag{3}$$

$$O(^1D) + H_2O \rightarrow 2\ {}^{\bullet}OH \tag{4}$$

$$O_3 + {}^{-}OH \rightarrow O_2^{-\bullet} + HO_2^{\bullet} \tag{5}$$

$$O_3 + HO_2^{\bullet} \rightarrow 2\ O_2 + {}^{\bullet}OH \tag{6}$$

$$O_3 + {}^{\bullet}OH \rightarrow O_2 + HO_2^{\bullet} \tag{7}$$

$$O_3 + O_2^{-\bullet} \rightarrow O_3^{-\bullet} + O_2 \tag{8}$$

$$O_3^{-\bullet} + H^+ \rightarrow HO_3^{\bullet} \tag{9}$$

$$HO_3^{\bullet} \rightarrow O_2 + {}^{\bullet}OH \tag{10}$$

Experiments of ozonation of t-BuOH alone (5.0×10^{-4} M) were carried out in our group at different pH values to verify under which conditions of pH ozone is efficiently converted into OH radicals. The results show that in ozonation experiments t-BuOH reacts only at pH 11, suggesting that at pH 1.8 and 7.0 no significant amounts of •OH are produced from ozone. Thus, we concluded that the conversion of t-BuOH observed in plasma treatment experiments at pH 1.8 and 7.0 is due to OH radicals produced directly by the discharge [11].

In this paper we report and discuss the results obtained in comparative experiments of ozonation and direct plasma treatment within the same experimental apparatus, the DBD reactor described previously [8]. For ozonation experiments the DBD discharge was kept off and ozone was produced by an external ozonizer and introduced into the reactor diluted within a flow of air to match the ozone concentration of the corresponding experiment with direct plasma treatment. This mode of operation is named *ex-situ* discharge as opposed to the *in-situ* discharge employed for direct plasma treatment. The experiments were performed using maleic acid and fumaric acid as test organic pollutants because their properties and reactivities are very well known in particular with regard to reaction with oxidants, including notably ozone and the hydroxyl radical [18–21]. This is not surprising since they are important degradation intermediates formed in the oxidation of phenol and of the majority of aromatic compounds [8, 22, 23]. The goal of this work was not so much to demonstrate the greater intrinsic efficacy of *in-situ* with respect to *ex-situ* discharge, but rather to take advantage of the extensive knowledge available on ozonation reactions to gain mechanistic insight into the plasma activated advanced oxidation, specifically about the relative contributions of OH radical and of ozone attack. The experimental degradation curves were matched by considering a simple kinetic model to verify the validity of the assumptions.

Experimental

Materials

Maleic and fumaric acids and H_2SO_4 were purchased from Sigma-Aldrich, $NaH_2PO_4{\cdot}H_2O$, $Na_2HPO_4{\cdot}12H_2O$, $Na_3PO_4{\cdot}12H_2O$, $NaHCO_3$, and Na_2CO_3 from Carlo Erba Reagenti. Ultrapure grade water (milliQ water) was obtained by filtration of deionized water with a Millipore system. Pure air used in the experiments was a synthetic mixture (80% nitrogen–20% oxygen) from Air Liquide with specified impurities of C_nH_m (< 0.5 ppm).

Experimental Apparatus

The experimental apparatus employed in the experiments was described in a previous report [6]. Briefly, the reactor is a glass vessel (internal dimensions 95 × 75 mm and 60 mm height) and has a teflon cover with four passing electrodes of stainless steel which support two parallel wires of 75 mm length and 0.15 mm diameter fixed upon their tips. The wires, made of stainless steel, are placed at a distance of 38 mm between each other and are kept above the aqueous solution. Volume and depth of the treated solution were 70 mL and 0.98 cm, respectively. The outside surface of the reactor base is covered with a film of silver and connected to a grounded plate. The reactor is powered with an AC high voltage transformer with 16.5–18 kV and a frequency of 50 Hz.

During the plasma treatment experiments, the voltage was maintained constant and voltage and current profiles were monitored with a digital oscilloscope (TDS5032B, bandwidth 350 MHz, sample rate 5 Gs/s) to assure the reproducibility of the electrical conditions. A flow of air of 30 mL min^{-1} was allowed through the reactor and the discharge occurred in the gas phase above the liquid surface. To minimize evaporation phenomena from the solution to be treated, the air was humidified to RH 100% by passing it through a water bubbler placed before the reactor.

During the ozonation experiments, the electrical discharge was left off and the reactor was used as a simple vessel. Ozone was produced by an ozonizer (GAIOFISH 100) and a flow of 30 mL min^{-1} of air containing 1050 ppm of ozone was allowed through the reactor. The solution was magnetically stirred.

Experimental Procedure

Solutions of maleic or fumaric acids 5.0×10^{-4} M and of their mixture (2.5×10^{-4} M each) were prepared in H_2SO_4 1.7×10^{-2} M (pH 1.8), $NaHCO_3$ 4.4×10^{-3} M (pH 7.0), Na_2CO_3 4.4×10^{-3} M (pH 10.0) and Na_2HPO_4/Na_3PO_4 2.5×10^{-2} M (pH 11.3). A volume of 70 mL was subjected to plasma treatment or ozonation. The efficiency of the decomposition process was determined by measuring the conversion of the acids as a function of treatment time. To this end, at desired reaction times a 0.5 mL aliquot of the treated solution was withdrawn and analyzed by HPLC (Shimadzu LC-10AT pump with a UV–Vis Shimadzu SPD-10 detector). A Zorbax-SB 150x4.6 i.d. mm column (Agilent Technologies) was used with aqueous phosphate buffer 20 mM at pH = 2 containing 1% acetonitrile as eluent. The elution was followed at 210 nm. Relative uncertainty on the measured concentration was estimated to be ± 2.5%.

In the case of ozonation experiments, to achieve an interaction of ozone with the organic compounds as similar as possible to that which takes place in the plasma-induced process,

the same reactor used in the experiments with plasma was employed, the concentration of ozone was adjusted to be equal to that produced by the DBD discharge (1050 ppm) and ozone was not bubbled into the solution but simply flowed above the water surface at the same flow rate employed in the experiments with plasma, while the solution was magnetically stirred.

Results and Discussion

Maleic and fumaric acids are geometrical isomers, characterized by similar but well distinct properties, especially with regard to acid dissociation equilibria and reactivity towards OH radicals and ozone. Relevant data for the work described here are summarized in Table 1. The relative contributions of the three possible species for maleic and fumaric acids (undissociated acid, mono-dissociated acid and fully dissociated acid) depend on the pK_a of the acid and on the solution pH.

The solution pH affects not only the speciation of the organic acids but also the lifetime and amounts of the reactive species present into the system during the plasma treatment. Therefore, the effect of the solution pH was investigated systematically by performing experiments in buffered solutions at pH 1.8, 7.0, 10.0 and 11.3, obtained, respectively, by addition of H_2SO_4, $NaHCO_3$, Na_2CO_3 and of a mixture of Na_2HPO_4 and Na_3PO_4. Sulphate ions SO_4^{2-} generated by the dissociation of sulphuric acid can be considered unreactive in the system in exam, while bicarbonate and carbonate ions are known quenchers of OH radicals [12, 20]. However, it was demonstrated previously in experiments with phenol as the organic contaminant, that, in the reactor used in this investigation, at pH around 7–8, the type and concentration of the buffer used does not affect significantly the degradation rate [9]. In contrast, experiments with t-BuOH show that carbonate 4.4×10^{-3} M used to obtain pH 10.0 does act as a competitor for OH radicals (data not shown). Indeed, the rate constant for the reaction of carbonate with OH radicals, equal to 3.9×10^8 M^{-1} s^{-1} [20], is about 50 times higher than that of bicarbonate.

To distinguish the role of ozone among the reactive species formed in the plasma-liquid system and involved in the process, the results obtained in plasma treatment

Table 1 Kinetic constants for reaction of maleic acid, fumaric acid and phenol in their various ionization states (undissociated, monoanion and dianion) with ozone and with OH radical

Compound	pK_a	k_{O_3} (M^{-1} s^{-1})			k_{OH} (M^{-1} s^{-1})
		Undissociated	Monoanion	Dianion	
Maleic acid	1.6, 6.1	1.4×10^3 [21]	4.2×10^3 [21]	~7×10^3 [21]	6×10^9 (pH 4–10.5) [20]
			1×10^3 [18]	5×10^3 (pH 6) [18]	
				2.4×10^4 [19]	
Fumaric acid	3.0, 4.4	8.5×10^3 [21]	2.65×10^4 (pH 3.1) [21]	~6.5×10^4 [21]	6×10^9 (pH 4–10.5) [20]
			6×10^3 (pH 2) [18]	1×10^5 (pH 5) [18]	
Phenol	9.9	1.3×10^3 [18]	1.4×10^9 [18]		8.41×10^9 (phenol) [24] 9.6×10^9 (phenoxide) [20]

were compared with those achieved in ozonation experiments. In ozonation experiments, the same reactor used in the experiments with plasma was employed and the concentration of ozone in air was adjusted to be equal to that produced by the DBD discharge (1050 ppm). Moreover, the ozone containing air was not bubbled into the solution but simply allowed to flow above the water surface at the same flow rate employed in the experiments with plasma, to achieve an interaction of ozone with water and with the organic compounds as similar as possible to that which takes place in the plasma-induced process. However, in the case of plasma treatment the effect of 'ion wind' was clearly evident on the water surface, thus mixing the solution, while, when ozonation was performed under static conditions, the decay of the organic compounds proceeded irregularly. For this reason, the ozonation experiments reported in the paper were all carried out by magnetically stirring the solution and it was assumed that the two mixing conditions have a comparable effect also in enhancing the contact surface between ozone and the solution.

Experimental Results

The experimental data relative to the degradation of maleic acid are shown in Fig. 1, in which relative concentrations C/C_0 (where C and C_0 are the residual and the initial concentrations, respectively) are plotted against the treatment time. The left-hand side panel refers to the plasma treatment, whereas the right-hand side panel refers to ozonation. The symbols are the experimental outcomes while the solid lines are the interpolating curves obtained from the best match between the data and the basic kinetic model presented in Sect. "Kinetic Model and Data Elaboration". A preliminary analysis revealed, indeed, that the experimental data cannot be fitted by a simple monoexponential decay, as was instead the case for all the organic pollutants previously tested in the present reactor [8–10, 25–27] and for most plasma-induced degradation processes described in the literature [28]. Thus, a simple but physically plausible model was developed, as described later.

From the experimental data reported in Fig. 1, the half-life time of the organic contaminant was obtained graphically for each experiment (Table 2). It is evident that the degradation rate of maleic acid increases in the order pH 1.8 < pH 7.0 ≈ pH 10.0 << pH 11.3, both in plasma treatment and ozonation. Moreover, comparing the half-life times obtained in plasma treatment and ozonation, it is evident that plasma is more efficient than ozonation under all pH conditions tested.

Taking into account the results obtained previously with t-BuOH [11], described in the introduction section, it is hypothesized that the decomposition of maleic acid induced by ozonation at pH 1.8 and 7.0 is due only to reaction of the acid with ozone, while at pH 11.0 the contribution of the reaction with OH radicals formed from the decomposition of ozone becomes prevalent. Considering that the rate constant of the reaction of $^{\bullet}OH$ with maleic acid is six orders of magnitude higher than that with ozone (Table 1), this conclusion explains why at pH 11.0 the decomposition of maleic acid proceeds faster than at acidic and neutral pHs (Table 2). On the contrary, the slight increase in the rate of the process observed at pH 7.0 with respect to pH 1.8 (Table 2) can be related to the different dissociation state of maleic acid at these two different pH values ($pK_{a1} = 1.6$, $pK_{a2} = 6.1$) as the rate constants of the reaction with ozone of the undissociated acid, the monoanion and the dianion (Table 1) are different: at pH 1.8 maleic acid is about half undissociated and half mono-dissociated, while at pH 7.0 it is almost completely doubly dissociated.

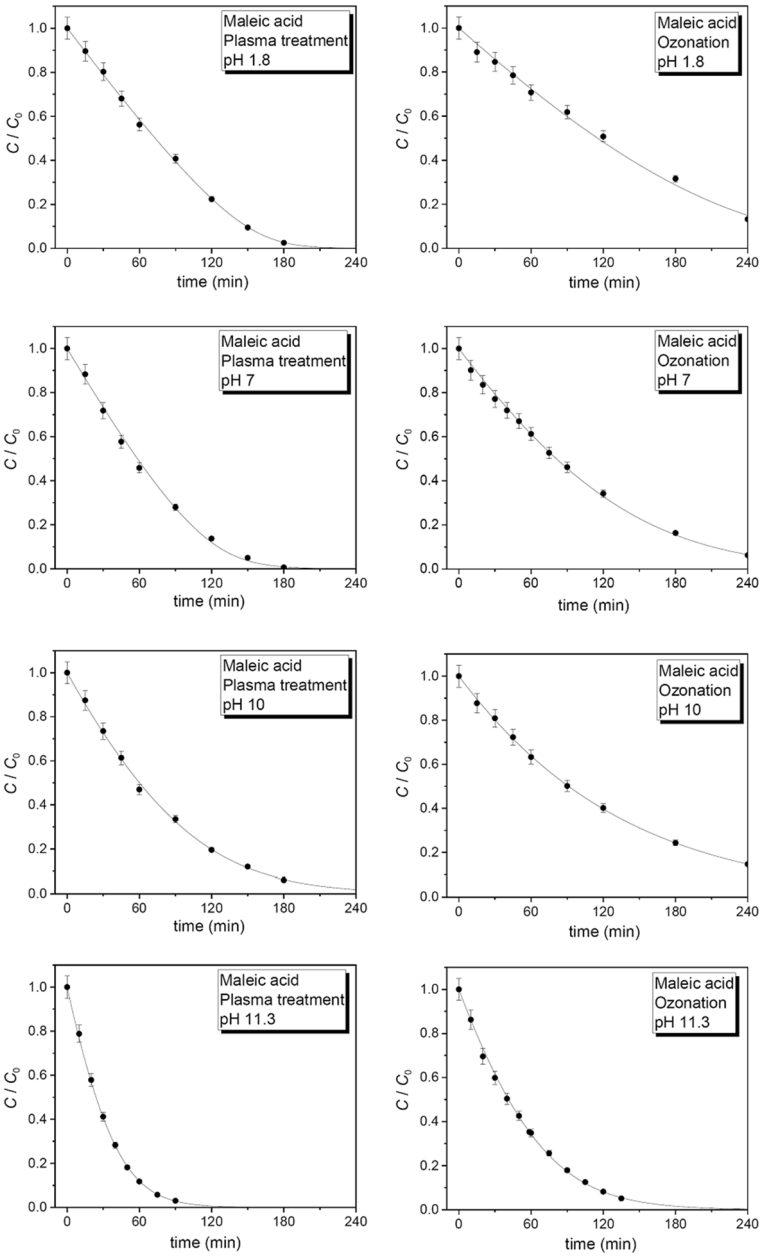

Fig. 1 Degradation of maleic acid (5×10^{-4} M) in aqueous solution at pH 1.8, 7.0, 10.0 and 11.3 by plasma treatment (left-hand side panels) and ozonation (right-hand side panels). The symbols are the experimental data points and the curves are the best fits using the model (see the text for details)

In the case of plasma treatment, the dependence of the process rate on pH is analogous to that observed in the case of ozonation. Considering that the reaction of $^{\bullet}$OH with maleic acid is independent on pH, it is concluded that the main contribution to the decomposition

Table 2 Observed half-life time for the degradation of maleic and fumaric acids treated individually in plasma and ozonation experiments under various pH conditions

Experimental conditions	$t_{1/2}$, min			
	Maleic acid		Fumaric acid	
	Plasma	Ozone	Plasma	Ozone
pH 1.8 (H_2SO_4 1.7×10^{-2} M)	70	110	45	73
pH 7.0 ($NaHCO_3$ 4.4×10^{-3} M)	62	79	15	29
pH 10.0 (Na_2CO_3 4.4×10^{-3} M)	59	87	24	27
pH 11.3 (Na_2HPO_4/Na_3PO_4 2.5×10^{-2} M)	24	40	24	25

of maleic acid induced by plasma at pH values of 1.8 and 7.0 is due to ozone; OH radicals participate to the oxidation process determining an increase in efficiency with respect to simple ozonation but are not responsible for the main process.

The results obtained at pH 10.0 deserve a special comment. Previous experiments allowed us to conclude that bicarbonate used in 4.4×10^{-3} M concentration to obtain pH 7.0 is not able to compete for OH radicals [9], whereas we have verified that carbonate, used at the same 4.4×10^{-3} M concentration to obtain pH 10.0, does act as a competitor for OH radicals (not shown). This competition thus explains why the results obtained at pH 10, in the HCO_3^-/CO_3^{2-} buffer, both in ozonation and plasma treatment, differ significantly from those obtained at pH 11.3, in the HPO_4^{2-}/PO_4^{3-} buffer, also if the dissociation state of maleic acid is the same at these two pH values. In the experiments at pH 10, therefore, the rate of maleic acid degradation is affected by the effective competition for OH radicals by one of the buffer species. These results highlight the complexity of pH effects in this system, specifically showing the interplay between effects on substrate reactivity, by determining its ionization state, and on reactive species distribution and density.

The oxidative removal of fumaric acid induced by plasma treatment and by ozonation at different pH values is shown in Fig. 2. As in the case of maleic acid, degradation induced by plasma treatment is faster than ozonation. This can be seen in Table 2 but at pH 10.0 and 11.3 half-life times obtained in plasma and ozonation are not significantly different. However, evidence that plasma treatment is faster than ozonation is found considering the residual concentration of fumaric acid after 60 min, which in the case of ozonation is twice that obtained in plasma treatment. The order of reactivity as a function of pH, based on fumaric acid half-life time, is pH 1.8 < pH 7.0 ≈ pH 10.0 ≈ pH 11.3 in both plasma treatment and ozonation. This order reflects the ionization state of fumaric acid which is undissociated at pH 1.8 while it is completely dissociated at pH 7.0, 10.0 and 11.3 ($pK_{a1} = 3.0$, $pK_{a2} = 4.4$). As in the case of maleic acid, the higher decomposition rates obtained in the oxidation induced by plasma can be ascribed to the additional contribution of OH radicals produced by the electrical discharge. On the contrary, at pH 11.3 the conversion of ozone to $^{\bullet}OH$ does not induce any significant increase in the decomposition rate of fumaric acid either in ozonation or in plasma treatment, as is instead observed in the case of maleic acid. This can be ascribed to the higher reactivity of fumaric acid with ozone with respect to that of maleic acid (Table 1), probably making the contribution of attack by ozone equally important as that by OH radicals.

Degradation of maleic and fumaric acid induced by plasma treatment and ozonation was then studied using a 1:1 mixture of the two compounds. It is known that the decomposition efficiency of a compound treated individually in a plasma system depends on its

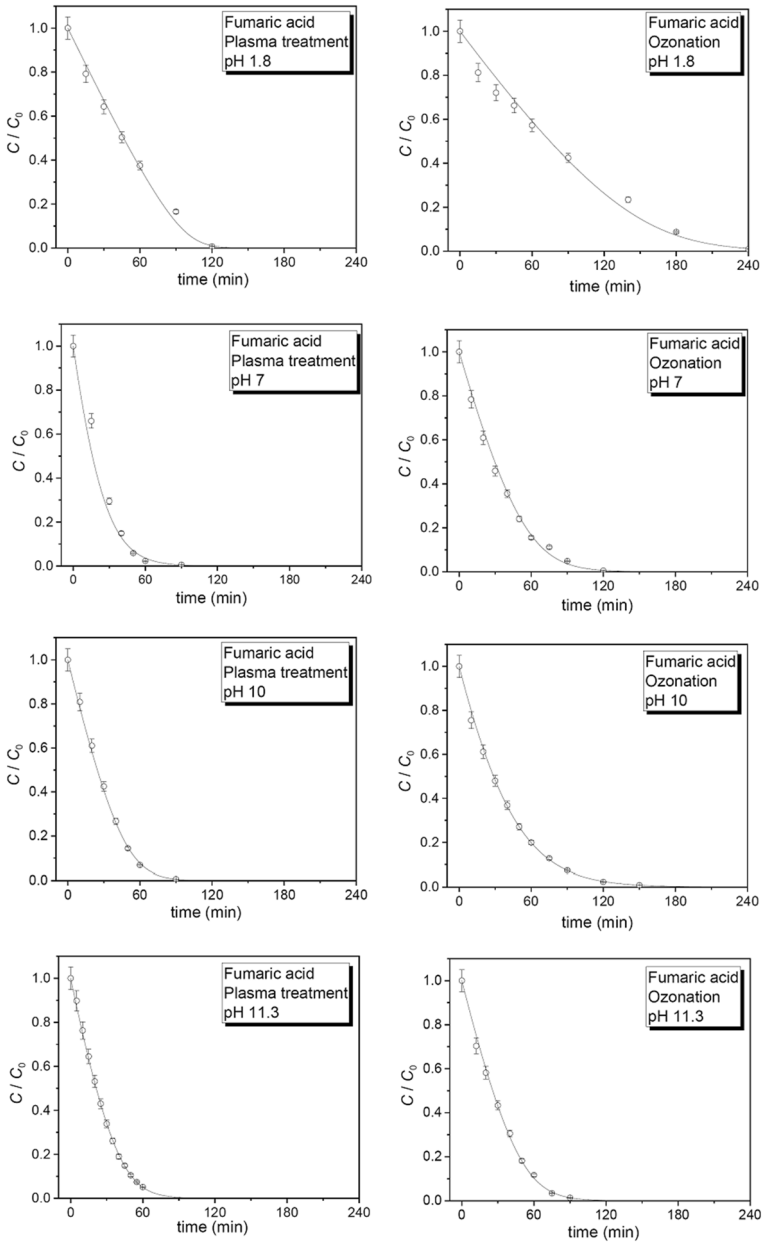

Fig. 2 Degradation of fumaric acid (5×10^{-4} M) in aqueous solution at pH 1.8, 7.0, 10.0 and 11.3 by plasma treatment (left-hand side panels) and ozonation (right-hand side panels). The symbols are the experimental data and the curves are the best fits using the model (see the text for details)

initial concentration, C_0, the rate usually decreasing with increasing C_0. This phenomenon is due to competition for the reactive species by reaction products/intermediates generated from the original compound [25] and is to be taken in due consideration when

comparing the reactivity of a compound measured when treated alone and in mixture [29]. In the experiments performed with mixtures of maleic and fumaric acids, the initial concentration of each of the compounds was thus halved with respect to the experiments in which each was treated as single component. In general, when two compounds are treated in mixture three different scenarios are possible:

(i) the two organic compounds react with different oxidizing species, thus they do not influence each other. The kinetic constants obtained in the experiments in mixture are equal to those obtained when the compounds are treated individually at the same initial concentration;
(ii) the two organic compounds react with the same oxidizing species, thus their competition for it (or them) can be evaluated by comparing the rates observed in the experiments carried out with mixtures with those obtained in experiments carried out with single compounds, each treated at a double initial concentration than used in the mixtures. Specifically, the rate of reaction observed for compound **A** when treated in mixture with **B**, each with an initial concentration of 2.5×10^{-4} M (competition between Compound **A** 2.5×10^{-4} M + Compound **B** 2.5×10^{-4} M), was compared with that observed when **A** was treated alone at an initial concentration of 5.0×10^{-4} M (a situation which can be viewed in this context as a "self-competition", i.e. Compound **A** 2.5×10^{-4} M + Compound **A** 2.5×10^{-4} M). Similarly for compound **B**;
(iii) the decomposition efficiency of the organic compounds increases or decreases when they are treated in mixture because one of them or a species originating from one of them reacts with the other.

Due to the very similar structures of maleic and fumaric acids and to the available data on their reactions with ozone and OH radicals (Table 1), case (ii) is expected.

The decomposition curves obtained in the experiments of plasma treatment and ozonation of the 1:1 mixture of maleic and fumaric acids are reported in Fig. 3.

It can be seen that at pH 1.8 and 7.0 the concentration vs reaction time profiles of these acids change dramatically when they are treated in mixture: in particular, the decomposition of maleic acid shows an induction period in which its reaction is slowed down by the presence of fumaric acid followed by an acceleration when fumaric acid has been largely degraded. At first, the hypothesis of an isomerization reaction between the two compounds was considered to explain this particular behavior, but ruled out since no significant amount of the other isomer was detected in the experiments performed with only one of the acids. Moreover, in the literature it is reported that ozonation does not induce the isomerization of maleic and/or fumaric acid in water [21]. The data were thus interpreted considering the model presented in Sect. "Kinetic Model and Data Elaboration".

The unusual competition effect observed for the mixture was never seen before in experiments with mixtures of organic compounds treated together in this reactor or in a companion larger prototype (7-wires) [10, 29]. To gain insight into this peculiar behavior observed with maleic and fumaric acids, additional competition experiments were run in which each was treated in equimolar mixture with phenol, which, as stated before, is the prototypal organic pollutant used to test advanced oxidation processes in general and, specifically, our plasma reactors. The results, reported in Fig. 4, show regular decay for all treated compounds with no evidence, specifically, of an initial induction period in the reaction of maleic acid.

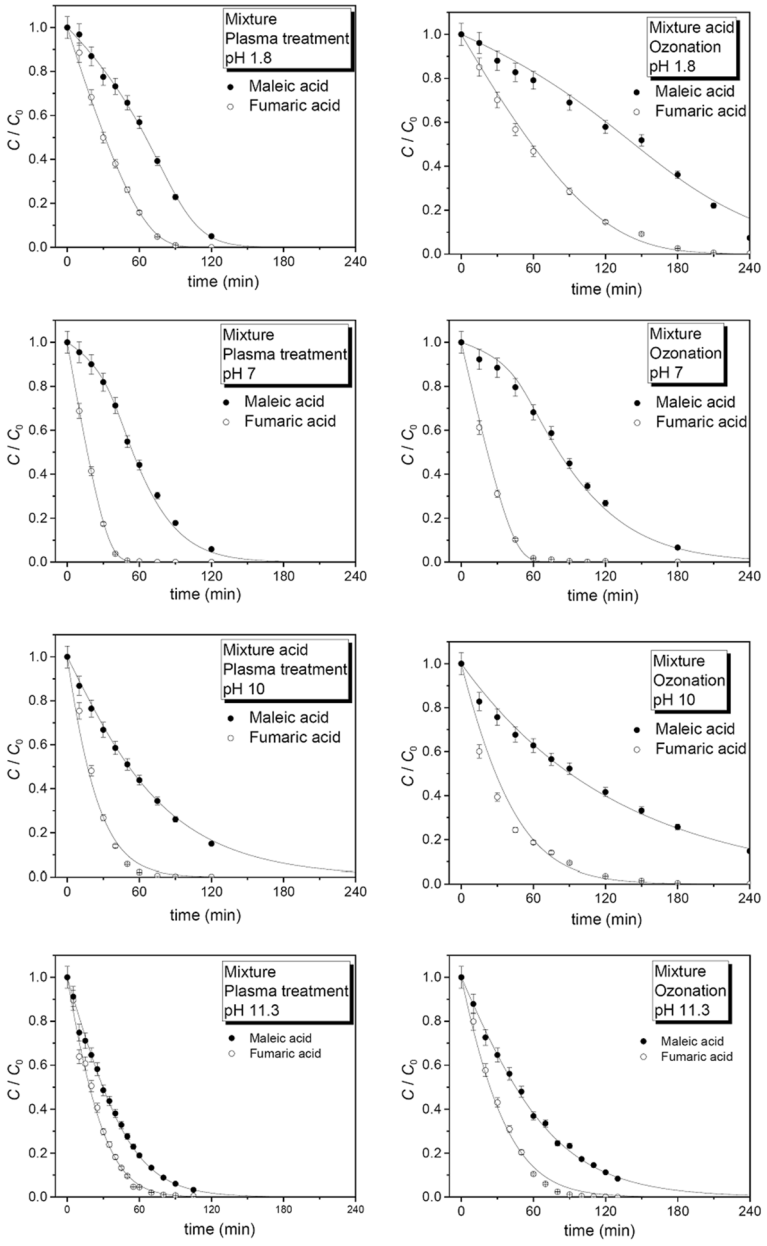

Fig. 3 Degradation of a 1:1 mixture of maleic and fumaric acids (2.5×10^{-4} M each) in aqueous solution at pH 1.8, 7.0, 10.0 and 11.3 by plasma treatment (left-hand side panels) and ozonation (right-hand side panels). The symbols are the experimental data (full circles for maleic acid, empty circles for fumaric acid) and the curves are the best fits using the model (see the text for details)

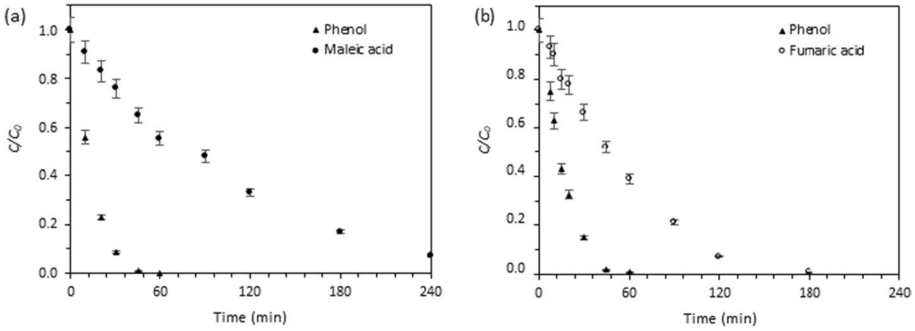

Fig. 4 Plasma treatment of equimolar mixtures of: **a** phenol and maleic acid (each 2.5×10^{-4} M) and **b** phenol and fumaric acid (each 2.5×10^{-4} M) in aqueous solution at pH 7.0

Kinetic Model and Data Elaboration

Kinetic Model

In order to account for the experimental profiles, a kinetic model was built on the basis of a few assumptions. Let V_g and V_l be the volumes of the gas and liquid phases, respectively, within the reactor. First, it is assumed that a reactive species X_g is produced at constant source rate S in the gas phase. Due to advection through the reactor, X_g has a certain residence time τ_g in the gas phase given by the ratio V_g/F_g, where F_g is the volumetric flow of gas phase. The species X_g is also transferred into the liquid phase. We assume that the mass transfer flow of X_g in the direction gas-to-liquid through the whole surface of contact (moles per unit of time) is proportional to the concentration of X_g in the gas phase, with an effective proportionality coefficient ρ_{gl} (having physical dimensions of volume over time) that depends on the physical mechanism of transfer and on the area of the contact surface. In the liquid phase, the species can persist as X_g and react with the compound M or it can quickly and quantitatively convert into a different species that then reacts with M. Comprising both possibilities, such a reactive species is indicated with X. If X coincides with X_g, the species is allowed to return back into the gas phase and the mass-transfer flow through the whole contact surface is assumed proportional to the concentration of X_g in the liquid phase with proportionality coefficient ρ_{lg}. On the contrary, if X differs from X_g, the transfer into the gas phase is ignored (i.e., $\rho_{lg} = 0$ in what follows) or possibly incorporated in the irreversible decomposition ("global sink process") of X.

As pointed out in "Appendix A", the effective coefficients ρ_{gl} and ρ_{lg} depend on the geometry of the reactor (both are proportional to the contact area A between gas and liquid), on the operative modality, and on some physico-chemical properties of X_g in the gas and liquid phases at the interface. Note that, at the level of our basic model, the kind of the transfer mechanism is not specified (although the transfer via diffusion in stagnant films is the most plausible one, at least in the ozonation modality). Therefore, a specific interpretation of ρ_{gl} and ρ_{lg} is not required, provided that the rate Eqs. (A1) and (A2) are applicable.

In solution, the species X attacks M according to $M + X \rightarrow \ldots$ where the dots stand for a product species that can further react with X generating a cascade of other intermediates each reacting with X up to a termination process. Finally, it is assumed that X is irreversibly quenched via a first-order process. Figure 5 depicts the global scheme and

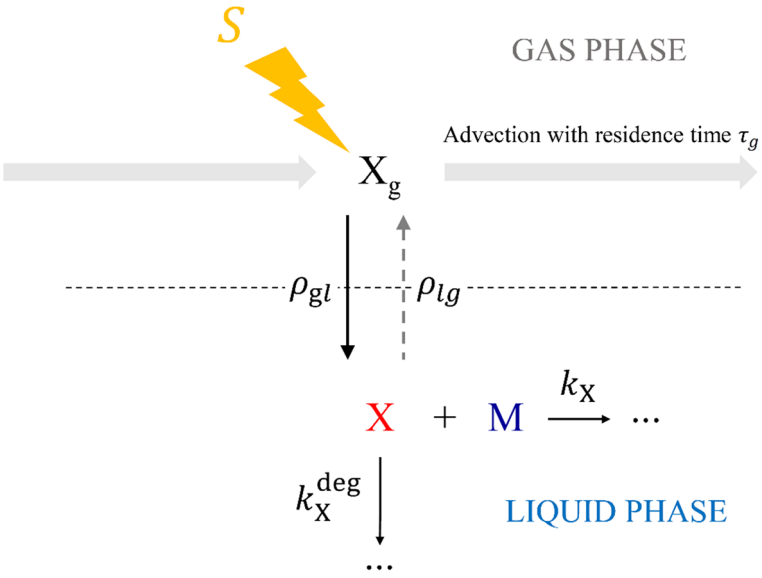

Fig. 5 The kinetic scheme. The species X (the reactive species in solution) can coincide with X_g produced in the gas phase or can be a different species which is quickly and quantitatively generated from X_g in solution. In the latter case, the transfer coefficient from liquid phase to gas phase (ρ_{lg}) has to be set equal to zero. The dots stand for intermediate species or waste products that are irrelevant in the model

sets the notations. In the modelling it is assumed that steady-state conditions are rapidly attained for both X in solution and X_g in the gas phase.

The details of the model are provided in the Appendix. In what follows we summarize the outcomes of the elaboration, distinguishing the case of a single species M (i.e., fumaric acid alone or maleic acid alone) from the case of mixtures of two species M_A and M_B.

Degradation of Single Species

Let *C(t)* be the volumetric (molar) concentration of the species M at time *t*, and C_0 its initial concentration. As shown in the first section of Appendix A, the evolution of *C(t)* is approximately described by the following differential equation:

$$\frac{dC(t)}{dt} = -\frac{\sigma\, C(t)}{1 + \varepsilon\, C(t)} \tag{11}$$

where σ and ε, which have physical dimensions of an effective rate constant and of an inverse-of-concentration, respectively, turn out to be related to the kinetic parameters of the model (see Fig. 5) as follows:

$$\sigma = \frac{k_X\, \tau_g\, \rho_{gl}}{\rho_{lg} + k_X^{deg}\, V_l\left(1 + \tau_g \rho_{gl}/V_g\right)} S \tag{12}$$

and

$$\varepsilon = \frac{k_X\, V_l\left(1 + \tau_g \rho_{gl}/V_g\right)}{\rho_{lg} + k_X^{deg}\, V_l\left(1 + \tau_g \rho_{gl}/V_g\right)} \tag{13}$$

Note that both σ and ε linearly depend on the degradation rate constant k_X, and that σ is also proportional to the source rate S. The integration of Eq. (11) yields the following equation that implicitly specifies the concentration $C(t)$ at the generic time:

$$\varepsilon\, \left[C_0 - C(t)\right] - \ln \frac{C(t)}{C_0} = \sigma\, t \tag{14}$$

Equation (14) tells us that the temporal decay of C is not monoexponential. The simple mono-exponential decay is obtained only in the limit $C_0 \ll \varepsilon^{-1}$. In other words, if one tries to fit the profile of C versus t with a monoexponential decay, the procedure would yield an apparent C_0-dependent effective decay rate that asymptotically tends to level off to the value σ as C_0 is smaller and smaller. However, it is interesting to note that an approximate monoexponential decay is always predicted for the long-time limit tail regardless of the value of ε. Indeed, in the long-time limit the approximate solution of Eq. (14) is $C(t) \cong C_0 e^{\varepsilon C_0} e^{-\sigma t}$.

The effectiveness of Eq. (14) has been tested for fumaric and maleic acids under the various pH conditions, both for ozonation and plasma treatment. In each case, the best parameters ε and σ have been determined by means of a 'fitting procedure' based on the minimization of an objective function (OF) built on the basis of the experimental data taking the summation of the squares of the difference between the two members of Eq. (14) at each time. The best estimates of ε and σ have been obtained by means of a scan on a grid of values.

Table 3 collects the best values of ε and σ obtained for each of the experimental conditions. We do not provide uncertainties on the parameters since the fitting procedure implemented here is unconventional and an objective quantitative assessment of the likelihood has still to be devised. What can be said is that the objective function revealed to be very sensitive to the variation of σ, but less sensitive to the variation of ε. This means that σ is determined in

Table 3 Parameters σ and ε from the best matching between model and experimental data for the degradation of single species (fumaric acid 5×10^{-4} M or maleic acid 5×10^{-4} M) by means of plasma treatment or ozonation at several pH values

pH	σ of maleic acid (min^{-1})	ε of maleic acid (M^{-1})	σ of fumaric acid (min^{-1})	ε of fumaric acid (M^{-1})
Plasma treatment				
1.8	0.060	1.5×10^4	0.11	1.8×10^4
7.0	0.052	9.4×10^3	0.068	1.5×10^3
10.0	0.022	2.4×10^3	0.087	5.8×10^3
11.3	0.051	2.1×10^3	0.086	4.5×10^3
Ozonation				
1.8	0.016	4.8×10^3	0.033	7.0×10^3
7.0	0.016	2.5×10^3	0.060	4.3×10^3
10.0	0.0087	3.9×10^2	0.036	1.3×10^3
11.3	0.028	1.9×10^3	0.074	4.8×10^3

a relatively sharp way, while a greater uncertainty is expected to bear on ε. A proper sensitivity analysis with respect to σ and ε, and also with respect to the form of the OF, is beyond the scope of this work whose main goal is showing that a minimal kinetic model can explain the experimental trends with few effective parameters. With ε and σ at disposal, Eq. (14) was then employed to generate the best-matching profiles of $C(t)/C_0$ shown in Figs. 2 and 3. As can be seen, there is a qualitative well matching between the experimental data and calculated profiles also taking into account the experimental error bars.

Since σ is proportional to k_X, it could be expected that σ values reflect the trend of $t_{1/2}$ reported in Table 2 because the experimental setup is the same in all cases (and under the assumption that the mass-transfer coefficients ρ_{gl} and ρ_{lg} are nearly the same under all conditions tested). Namely, although the kinetic law is not a simple first-order decay, it is expected that lower $t_{1/2}$ are associated with higher σ values. Effectively, the σ values relative to experiments with fumaric acid are all higher than those obtained with maleic acid carried out under the same conditions, and σ values relative to experiments of ozonation are all lower than in the corresponding experiments of plasma treatment. On the other hand, the σ values obtained under different pH conditions do not follow the observed monotonic order of reactivity deduced from $t_{1/2}$. Unfortunately, the uncertainty that bears on σ, and the fact that the values are relatively close to each other, do not allow us to establish if the non-monotonic trend of the σ values is a real (physical) fact or if it is merely due to the limits of the fitting procedure. However, the important fact to note is that our basic two-parameter model fits well the experimental data. This leads us to believe that the underlying hypotheses are valid, in particular that at a given pH only one main reactive species is active.

Binary Mixtures

In the case of the binary equimolar mixture of maleic and fumaric acids, indicated as M_A and M_B, under the assumptions made in Sec. "Experimental Results", the evolution of the concentrations can be described by the following system of differential equations:

$$\begin{aligned}\frac{dC_A(t)}{dt} &= -\frac{\sigma_A\, C_A(t)}{1+\varepsilon_A\, C_A(t)+\varepsilon_B\, C_B(t)}\\ \frac{dC_B(t)}{dt} &= -\frac{\sigma_B\, C_B(t)}{1+\varepsilon_A\, C_A(t)+\varepsilon_B\, C_B(t)}\end{aligned} \tag{15}$$

where the parameters σ_A and σ_B are defined exactly as in Eq. (12) with reference to the M_A and M_B reactants, while the parameters ε_A and ε_B are defined as in Eq. (13). The integration of Eqs. (15) is analytical. For the sake of notation, the dimensionless quantities $x_A(t) = C_A(t)/C_{A,0}$ and $x_B(t) = C_B(t)/C_{B,0}$ are introduced. In the second section of Appendix A it is shown that x_A is implicitly defined, at each time, through the following equation

$$\varepsilon_A\, C_{A,0}\left(1-x_A\right) - \ln x_A + \varepsilon_A C_{B,0}\left(1-x_A^{\sigma_B/\sigma_A}\right) = \sigma_A\, t \tag{16}$$

and that the companion quantity x_B is given by

$$x_B = x_A^{\sigma_B/\sigma_A} \tag{17}$$

Ultimately, three parameters have to be determined from the best-matching with the experimental data: ε_A, σ_A and σ_B. As for the solutions of single compounds, these

parameters have been determined through the minimization of an objective function built with the experimental data. With ε_A, σ_A and σ_B at disposal, Eqs. (16)–(17) were used to generate the profiles of $C_A(t)/C_{A,0}$ and $C_B(t)/C_{B,0}$. Clearly, the assignment of the labels 'A' and 'B' to fumaric or maleic acid is irrelevant (in the numerical analysis here performed, 'A' was assigned to fumaric acid and 'B' to maleic acid). Table 4 collects the parameters obtained from the best-matching route. We must stress that the uncertainty on the 'fitting' outcomes is here much higher than in the case of the single species since the number of parameters was increased from two to three. As a consequence, the outcomes show an irregular trend and high variations that make it difficult to attribute a change of σ and/or ε exclusively to the different experimental conditions. In spite of this, some qualitative and provisional argumentations can be made.

Figure 3 shows that the experimental data are qualitatively well-matched by the developed model, also considering the experimental error bars. This means that, to explain the S-shape of the degradation curve of maleic acid observed at pH 1.8 and 7.0 both in plasma treatment and ozonation, it is not necessary to consider additional processes (e.g. isomerization) possibly taking place into the system besides the ones reported in Fig. 5. Moreover, the observation of the S-shape of the maleic acid curves is observed under the two pH conditions, pH 1.8 and 7.0, in which the main reactive species is considered to be the same, i.e. ozone, as discussed in Sect. "Experimental Results", reinforcing the hypothesis itself. When treated in mixture, maleic and fumaric acid compete for ozone, which is evidently in large defect with respect to the reactants, and fumaric acid prevails in the competition thanks to its higher reactivity with ozone (Table 1). Comparing plasma treatment and ozonation at the same pH, degradation is faster in plasma treatment than in ozonation and, accordingly, σ_M and σ_F are higher in plasma treatment; this can be explained, as in the case of experiments with the single compounds, considering the contribution to the oxidation activated by plasma due to OH radicals produced by the electrical discharge.

At pH 11.3 the decomposition of ozone into OH radicals, which react at the same rate with maleic and fumaric acids, induces a change in the shape of the degradation curve of maleic acid. However, if $^{\bullet}$OH were the only reactive species, the same degradation rate would be observed for the two acids. The fact that maleic acid is degraded more slowly evidences some contribution by O_3 also at basic pH.

At pH 10.0, the competition of carbonate for the OH radical complicates further the system. The rather large difference in reactivity observed between maleic and fumaric acids indicates a strong contribution of ozone, while the higher reactivity of both acids in plasma

Table 4 Parameters σ and ε from the best-matching between model and experimental data for the degradation of a 1:1 binary mixture of fumaric acid (subscript 'F') 2.5×10^{-4} M and maleic acid (subscript 'M') 2.5×10^{-4} M by means of plasma treatment or ozonation at several pH values

pH	σ_M (min^{-1})	ε_M (M^{-1})	σ_F (min^{-1})	ε_F (M^{-1})
Plasma treatment				
1.8	0.076	1.2×10^4	0.24	3.8×10^4
7.0	0.045	4.7×10^3	0.40	4.2×10^4
10.0	0.017	4.8×10^2	0.058	1.7×10^3
11.3	0.040	1.7×10^3	0.070	2.9×10^3
Ozonation				
1.8	0.017	4.8×10^3	0.064	1.8×10^4
7.0	0.025	3.5×10^3	0.32	4.6×10^4
10.0	0.0077	10	0.030	40
11.3	0.022	9.7×10^2	0.046	2.0×10^3

treatment with respect to ozonation indicates that carbonate competes for OH radicals but does not completely quenches them.

In conclusion, the simple model adopted here achieved a remarkable fit of all experimental data in spite of its simplifying assumptions, such as the attainment of stationary conditions. For instance, the details of the mass transfer at the gas–liquid interface are not here taken into account in detail, whereas several studies stressed the importance of considering the occurrence of chemical reactions both in the surface film and in the bulk liquid phase [30, 31], and of focusing on the interplay between chemical reaction and mass-transfer rate [32]. Interestingly, the assumption of a single reactive species proved effective as a work hypothesis, despite the fact that both ozone and OH radicals are expected to be involved in these processes. This leads to the interesting conclusion that, depending on the pH conditions, one reactive species prevails, ozone under acidic conditions and OH radicals under basic conditions. The results of competition experiments with phenol are consistent with this proposal (Fig. 4). It is seen indeed that the degradation of maleic acid carried out in the presence of an equimolar amount of phenol does not show an induction period, as is found instead in competition experiments with fumaric acid. This is because the main route of phenol degradation does not involve attack by ozone but by OH radicals [11]. So, while fumaric acid competes very effectively with maleic acid for ozone, phenol does not. In Table 1 rate constants for reaction of undissociated phenol and of phenoxide anion with O_3 and $^{\bullet}OH$ are reported. Interestingly, at acidic pH phenol reactivity is very similar to that of maleic acid but its rate constant with OH radical is instead significantly higher than that of maleic and fumaric acids.

Conclusions

The following conclusions can be drawn:

- it is demonstrated that, with respect to ozonation, direct plasma treatment achieves faster oxidation of maleic acid and fumaric acid, an effect attributed to the possible engagement of OH radicals produced by the discharge in addition to those derived from ozone itself;
- under all conditions tested, fumaric acid is more reactive than maleic acid. Since both react with OH radicals at the same rate, whereas the reaction with ozone is faster for fumaric acid than for maleic acid, the important role of direct attack by ozone in bringing about the degradation of both compounds under acidic and neutral pH conditions is unveiled;
- the prevalent role of direct attack by ozone under acidic and neutral pH conditions is also evident in the results of experiments in which maleic and fumaric acids were treated together in equimolar amounts, showing an induction period for the reaction of maleic acid;
- a simple kinetic model was developed, based on the assumptions, among others, that steady-state conditions are rapidly attained and that a single reactive species is responsible for the degradation of the compounds in solution. In spite of its simplicity, the model proved capable of accounting for the experimental data, suggesting that the relevant physical features of the process are captured. Specifically, it supports the conclusion that, depending on the solution pH one reactive species prevails, ozone under acidic conditions and OH radicals under basic conditions;

- The results of competition experiments with phenol provide support for the conclusion that direct attack by ozone is important in the degradation of both maleic and fumaric acids in experiments of plasma treatment at neutral pH. Thus, no induction period was observed in the reaction of either maleic or fumaric acids treated in competition with phenol, a compound which was shown earlier to react via prevalent attack by OH radicals [11].

Appendix A

Degradation of Single Species

Let us indicate with X_g the reactive species introduced/produced in the gas phase with a given source rate S, and let X be the reactive species that in solution does degrade the compound M (either maleic or fumaric acid). Let us bear in mind that X_g and X might be the same species, or X_g could be the precursor of X; in the latter instance, we assume that X is immediately generated by X_g as soon as X_g passes from the gas phase to the solution.

Following the conventional notation, let us adopt square brackets to indicate the volumetric concentration of a species. Under the assumption of well-mixed bulk phases, we can adopt standard mass-action rate equations for the evolution of the concentrations. By taking into account the kinetic processes sketched in Fig. 5 (to which we address for the notation), the rate equations for the reactive species read

$$\frac{d[X_g]}{dt} = S - \frac{[X_g]}{\tau_g} - \frac{\rho_{gl}}{V_g}[X_g] + \frac{\rho_{lg}}{V_g}[X] \tag{A1}$$

and

$$\frac{d[X]}{dt} = \frac{\rho_{gl}}{V_l}[X_g] - \left(\frac{\rho_{lg}}{V_l} + k_X^{deg} + k_X[M]\right)[X] \tag{A2}$$

The transfers of the reactive species from gas to liquid, and viceversa, are treated as first-order processes. The division of the last two terms on the right-hand-side of Eq. (A1) by V_g (volume of the gas phase) is required for turning from the quantity of species transferred through the whole gas–liquid contact surface per unit of time, to the associate rate of variation of the concentration in the gas phase. Similarly, the division by V_l (volume of the liquid phase) is required in the corresponding terms on the right-hand-side of Eq. (A2). Let us recall that the coefficient ρ_{lg} has to be set equal to zero if X differs from X_g. The contribution $-[X_g]/\tau_g$ that enters Eq. (A1) corresponds to the removal by advection due to the flowing of the gas phase through the reactor. Here, τ_g is the residence time of X_g in the gas phase under stationary conditions.

Concerning the mass-transfer terms, the effective parameters ρ_{gl} and ρ_{lg} depend on reactor's geometry (both are proportional to the gas–liquid contact area A), on the operative modality, and are specific of X_g. Note that our model is generic and an interpretation of ρ_{gl} and ρ_{lg} is not required. In particular, the physical nature of the transfer mechanism is not specified, although the transfer via diffusion in stagnant films is the most plausible one, at least in the ozonation modality. In such case, according to standard models of transfer in multimedia systems under steady-state conditions, ρ_{gl} and ρ_{lg} would be given, respectively, by A divided by the global resistances of the double-layer from gas to liquid and from

liquid to gas, R_{gl} and R_{lg}, which are determined by the diffusion coefficients of X_g in the gas and liquid stagnant films, by the thickness of the films, and by the partition constant of X_g between the two phases.

Concerning the source rate S of X_g in the gas phase, in the ozonation modality the species is introduced with a given concentration $[X_g]_{in}$, hence $S = F_g\,[X_g]_{in}$ where F_g is the volumetric flow of the gas phase. In the plasma modality, S is controlled the setup parameters of the plasma generation. In writing Eq. (A2) we are implicitly neglecting the possible intermediate species that are produced by the reaction of X with M and that further react with X up to a termination process. For the degradation of M in solution we have

$$\frac{d[\mathrm{M}]}{dt} = -k_{\mathrm{X}}[\mathrm{M}][\mathrm{X}] \tag{A3}$$

Let us assume that (quasi) stationary conditions are attained for both X_g in the gas phase and X in solution. This corresponds to assume that the concentrations of X_g and X rapidly follow the slower evolution of the concentration of M. Such assumption is expected to be licit as long as some of the creation/loss processes of X are much faster than the degradation of M. With this working position, the quasi-stationary concentrations $[X_g]$ and [X] are obtained setting $d[X_g]/dt = 0$ and $d[X]/dt = 0$ in Eqs. (A1) and (A2). Then, by substituting [X] into Eq.(A3), and recalling the parameters σ and ε defined in Eqs. (12) and (13), the effective rate equation Eq. (11) is obtained.

Degradation of Binary Mixtures

The elaboration made in the first section of the Appendix can be straightforwardly adapted to the case of two compounds M_A and M_B that are simultaneously degraded in solution. The rate equation (A2) is now replaced by

$$\frac{d[\mathrm{X}]}{dt} = \frac{\rho_{gl}}{V_l}[\mathrm{X}_g] - \left(\frac{\rho_{lg}}{V_l} + k_{\mathrm{X}}^{\mathrm{deg}} + k_{\mathrm{X}}^{\mathrm{A}}[\mathrm{M_A}] + k_{\mathrm{X}}^{\mathrm{B}}[\mathrm{M_B}]\right)[\mathrm{X}] \tag{A4}$$

and two degradation processes have to be taken into account:

$$\frac{d[\mathrm{M_A}]}{dt} = -k_{\mathrm{X}}^{\mathrm{A}}[\mathrm{M_A}][\mathrm{X}], \quad \frac{d[\mathrm{M_B}]}{dt} = -k_{\mathrm{X}}^{\mathrm{B}}[\mathrm{M_B}][\mathrm{X}] \tag{A5}$$

By assuming quasi-stationary condition for X_g and X, and substituting the resulting concentration [X] in Eq. (A5), the effective rate equations for the evolution of $[M_A]$ and $[M_B]$ are derived. Using the scaled quantities $x_A = [M_A]/[M_A]_0$ and $x_B = [M_B]/[M_B]_0$, the rate equations read

$$\frac{dx_{\mathrm{A}}(t)}{dt} = -\frac{\sigma_{\mathrm{A}}\,x_{\mathrm{A}}(t)}{1 + \alpha_{\mathrm{A}}\,x_{\mathrm{A}}(t) + \alpha_{\mathrm{B}}\,x_{\mathrm{B}}(t)} \tag{A6}$$

and

$$\frac{dx_{\mathrm{B}}(t)}{dt} = -\frac{\sigma_{\mathrm{B}}\,x_{\mathrm{B}}(t)}{1 + \alpha_{\mathrm{A}}\,x_{\mathrm{A}}(t) + \alpha_{\mathrm{B}}\,x_{\mathrm{B}}(t)} \tag{A7}$$

where the effective rate parameters σ_A and σ_B are expressed exactly as in Eq. (12) using the specific kinetic rates for the compound M_A or M_B, respectively. For the sake of notation we

have introduced the dimensionless quantities $\alpha_A = \varepsilon_A [M_A]_0$ and $\alpha_B = \varepsilon_B [M_B]_0$, where the parameters ε_A and ε_B are expressed as in Eq. (13) for M_A or M_B.

The system of equations (A6) and (A7) can be elaborated by taking into account that $\sigma_A^{-1} d \ln x_A(t)/dt = \sigma_B^{-1} d \ln x_B(t)/dt = -[1 + \alpha_A x_A(t) + \alpha_B x_B(t)]^{-1}$, which implies $d \ln \left(x_A(t)^{1/\sigma_A} / x_B(t)^{1/\sigma_B} \right)/dt = 0$, hence the argument of the logarithm is conserved in time. Since its value at the time-zero is equal to 1, we get the following relationship between the two unknowns:

$$x_B(t) = x_A(t)^{\sigma_B/\sigma_A} \tag{A8}$$

This relation allows us to get rid of x_B. The insertion of Eq. (A8) into Eq. (A6) yields the following equation for x_A:

$$\frac{dx_A(t)}{dt} = -\frac{\sigma_A x_A(t)}{1 + \alpha_A x_A(t) + \alpha_B x_A(t)^{\sigma_B/\sigma_A}} \tag{A9}$$

By separating the variables we get $d[\ln x_A + \alpha_A x_A + \alpha_B(\sigma_A/\sigma_B) x_A^{\sigma_B/\sigma_A}] = -\sigma_A \, dt$. The integration between time-zero (at which $x_A(0) = 1$) and the generic time t yields

$$\alpha_A \left(1 - x_A\right) - \ln x_A + \alpha_B \frac{\sigma_A}{\sigma_B} \left(1 - x_A^{\sigma_B/\sigma_A}\right) = \sigma_A \, t \tag{A10}$$

Now, let us rewrite the factor $\alpha_B(\sigma_A/\sigma_B)$ as $\alpha_A \left[(\sigma_A/\alpha_A)/(\sigma_B/\alpha_B)\right]$, and hence as $\alpha_A \left([M_B]_0/[M_A]_0\right) \times \left[(\varepsilon_B/\varepsilon_A)(\sigma_A/\sigma_B)\right]$. Since $\varepsilon_B/\varepsilon_A = k_X^B/k_X^A$ (from Eq. (13) written for the compounds M_B and M_A and then taking the ratio) and $\sigma_A/\sigma_B = k_X^A/k_X^B$ (from Eq. (12) for M_B and M_A and taking the ratio), it follows that

$$\alpha_B \frac{\sigma_A}{\sigma_B} \equiv \alpha_A \frac{[M_B]_0}{[M_A]_0} = \varepsilon_A [M_B]_0 \tag{A11}$$

By using Eq. (A11) in Eq. (A10) we finally get Eq. (16).

Acknowledgements The stimulating environment provided by COST Action 19110 is gratefully acknowledged.

Authors' Contributions V.S. and E.C. performed the experimental work. D.F. carried out the kinetic modelling. E.M. and C.P. made conceptualization and supervision. The first draft of the manuscript was written by E.M, C.P. and D. F. All authors participated to data analysis and reviewed the manuscript.

Funding Open access funding provided by Università degli Studi di Padova. This work was funded by University of Padova (Grant P-DiSC#06BIRD2019-UNIPD).

Data Availability Data will be available on request.

Declarations

Competing interests The authors declare they have no financial or proprietary interests in any material discussed in this article.

Ethical Approval Not applicable.

References

1. Kogelschatz U (2003) Plasma Chem Plasma Process 23:1–46
2. von Sonntag C, von Gunten U (2012) Chemistry of ozone in water and wastewater treatment: from basic principles to applications. Iwa Publishing, London
3. Bruggeman P, Kushner M, Locke BR, Gardeniers J, Graham WG, Graves D, Hofman-Caris R, Marić D, Reid JP, Ceriani E, Fernández Rivas D, Foster J, Garrick J, Gorbanev Y, Hamaguchi H, Iza F, Jablonowski H, Klimova E, Kolb J, Krčma F, Lukeš P, Machala Z, Marinov I, Mariotti D, Mededovic Thagard S, Minakata D, Neyts E, Pawłat J, Petrović Z, Pflieger R, Reuter S, Schram D, Schröter S, Shiraiwa M, Tarabová B, Tsai P, Verlet J, von Woedtke T, Wilson K, Yasui K, Zvereva G (2016) Plasma Sources Sci Technol 25:053002
4. Vanraes P, Bogaerts A (2018) Appl Phys Rev 5:031103
5. Magureanu M, Bradu C, Parvulescu VI (2018) J Phys D Appl Phys 51:313002
6. Shang K, Li J, Morent R (2019) Plasma Sci Technol 21:043001
7. Takeuchi N, Yasuoka K (2021) Jpn J Appl Phys 60:00801
8. Marotta E, Schiorlin M, Ren X, Rea M, Paradisi C (2011) Plasma Process Polym 8:867–875
9. Marotta E, Ceriani E, Schiorlin M, Ceretta C, Paradisi C (2012) Water Res 46:6239–6246
10. Giardina A, Tampieri F, Biondo O, Marotta E, Paradisi C (2019) Chem Eng J 372:171–180
11. Tomei G, Saleem S, Ceriani E, Pinton A, Marotta E, Paradisi C (2023). Chem Eur J. https://doi.org/10.1002/chem.202302090
12. Hoigné J, Bader H (1976) Wat Res 10:377–386
13. Forni L, Bahnemann D, Hart EJJ (1982) Phys Chem 86:255–259
14. Glaze WH (1987) Environ Sci Technol 21:224–230
15. Sotelo JL, Beltrán FJ, Benitez JF, Beltrán-Heredia J (1987) Ind Eng Chem Res 26:39–43
16. Von Gunten U (2007) Water Sci Technol 55:25–29
17. Reisz E, Schmidt W, Schuchmann HP, von Sonntag C (2003) Environ Sci Technol 37:1941–1948
18. Bader H, Hoigné J (1983) Water Res 17:185–194
19. Pryor WA, Giamalva DH, Church DF (1984) J Am Chem Soc 106:7094–7100
20. Buxton GV, Greenstock CL, Helman WP, Ross AB (1988) J Phys Chem Ref Data 17:513–886
21. Leitzke A, von Stonnag C (2009) Ozone Sci Eng 31:301–308
22. Zazo JA, Casas JA, Mohedano AF, Gilarranz MA, Rodriguez JJ (2005) Environ Sci Technol 39:9295–9302
23. Lukes P, Dolezalova E, Sisrova I, Clupek M (2014) Plasma Sources Sci Technol 23:015019
24. Bonin J, Janik I, Janik D, Bartels DM (2007) J Phys Chem A 111:1869–1878
25. Marotta E, Ceriani E, Shapoval V, Schiorlin M, Ceretta C, Rea M, Paradisi C (2011) Eur Phys J Appl Phys 55:13811
26. Krishna S, Ceriani E, Marotta E, Giardina A, Špatenka P, Paradisi C (2016) Chem Eng J 292:35–41
27. Giardina A, Tampieri F, Marotta E, Paradisi C (2018) Chemosphere 210:653–661
28. Magureanu M, Bilea F, Bradu C, Hong D (2021) J Hazard Mat 417:125481
29. Tampieri F, Durighello A, Biondo O, Gąsior M, Knyś A, Marotta E, Paradisi C (2019) Plasma Chem Plasma Process 39:545–559
30. Benbelkacem H, Debellefontaine H (2003) Chem Eng Process 42:723–732
31. Benbelkacem H, Mathé S, Debellefontaine H (2004) Water Sci Technol 49:25–30
32. Bhosale GS, Vaidya PD, Joshi JB, Patil RN (2023) Ind Eng Chem Res 62:8181–8190